

Valence Anions in Complexes of Adenine and 9-Methyladenine with Formic Acid: Stabilization by Intermolecular Proton Transfer

Kamil Mazurkiewicz,[†] Maciej Harańczyk,[†] Maciej Gutowski,^{†,‡,§} Janusz Rak,^{*,†}
Dunja Radisic,[#] Soren N. Eustis,[#] Di Wang,[#] and Kit H. Bowen^{*,#}

Contribution from the Department of Chemistry, University of Gdańsk, Sobieskiego 18, 80-952 Gdańsk, Poland, Chemical Sciences Division, Pacific Northwest National Laboratory, Richland, Washington 99352, Department of Chemistry, School of Engineering and Physical Sciences, Heriot-Watt University, Edinburgh EH14 4AS, U.K., and Department of Chemistry, Johns Hopkins University, Baltimore, Maryland 21218

Received August 31, 2006; E-mail: janusz@raptor.chem.univ.gda.pl; kbowen@jhu.edu

Abstract: Photoelectron spectra of adenine–formic acid (AFA[−]) and 9-methyladenine–formic acid (MAFA[−]) anionic complexes have been recorded with 2.540 eV photons. These spectra reveal broad features with maxima at 1.5–1.4 eV that indicate formation of stable valence anions in the gas phase. The neutral and anionic complexes of adenine/9-methyladenine and formic acid were also studied computationally at the B3LYP, second-order Møller–Plesset, and coupled-cluster levels of theory with the 6-31++G** and aug-cc-pVDZ basis sets. The neutral complexes form cyclic hydrogen bonds, and the most stable dimers are bound by 17.7 and 16.0 kcal/mol for AFA and MAFA, respectively. The theoretical results indicate that the excess electron in both AFA[−] and MAFA[−] occupies a π^* orbital localized on adenine/9-methyladenine, and the adiabatic stability of the most stable anions amounts to 0.67 and 0.54 eV for AFA[−] and MAFA[−], respectively. The attachment of the excess electron to the complexes induces a barrier-free proton transfer (BFPT) from the carboxylic group of formic acid to a N atom of adenine or 9-methyladenine. As a result, the most stable structures of the anionic complexes can be characterized as neutral radicals of hydrogenated adenine (9-methyladenine) solvated by a deprotonated formic acid. The BFPT to the N atoms of adenine may be biologically relevant because some of these sites are not involved in the Watson–Crick pairing scheme and are easily accessible in the cellular environment. We suggest that valence anions of purines might be as important as those of pyrimidines in the process of DNA damage by low-energy electrons.

1. Introduction

Detailed knowledge of the mechanism of electron binding to nucleobases is crucial for understanding radiation damage to DNA. Low-energy electrons are formed as the dominant secondary species in the course of interaction between high-energy particles and water.¹ The seminal work of Sanche et al.² proved unequivocally that low-energy electrons induce a profound damage to DNA. The resonance structure of the damage quantum yield versus incident electron energy suggests that the resonance anions of nucleic acid bases (NBs) may play an important role in the mechanism of formation of strand breaks. Indeed, isolated nucleobases form shape resonances^{3,4} with positions close to the maximum of a sharp feature exhibited

by the single-strand breaks quantum yield versus incident electron energy.⁵

Although the resonant states seem to be formed at the very first stages of electron attachment to DNA, they might relax and convert into stable anions in subsequent steps of electron–molecule interactions.⁶ As a matter of fact, the most recent results from Bowen's group demonstrate that NBs support some anionic states characterized by electron vertical detachment energy (VDE) as large as 2.5 eV.⁷ Moreover, using the CCSD-(T) method, we showed that valence anions of pyrimidine bases, such as 1-methylcytosine,⁸ uracil,⁹ and thymine,¹⁰ with VDEs on the order of 2.5 eV, result from enamine–imine transformations; i.e., a proton is transferred between a NH site and a carbon site. Some of these valence anions proved to be adiabatically bound with respect to the most stable tautomers of neutral NBs.

[†] University of Gdańsk.

[‡] Pacific Northwest National Laboratory.

[§] Heriot-Watt University.

[#] Johns Hopkins University.

- (1) Abdoul-Carime, H.; Gohlke, S.; Fischbach, E.; Scheike, J.; Illenberger, E. *Chem. Phys. Lett.* **2004**, *387*, 267–270.
- (2) Boudaïffa, B.; Cloutier, P.; Hunting, D.; Huels, M. A.; Sanche, L. *Science* **2000**, *287*, 1658–1660.
- (3) Aflatooni, K.; Gallup, G. A.; Burrow, P. D. *J. Phys. Chem. A* **1998**, *102*, 6205–6207.
- (4) Burrow, P. D.; Gallup, G. A.; Scheer, A. M.; Denifl, S.; Ptasinska, S.; Märk, T.; Scheier, P. *J. Chem. Phys.* **2006**, *124*, 124310.

- (5) Martin, F.; Burrow, P. D.; Cai, Z.; Cloutier, P.; Hunting, D.; Sanche, L. *Phys. Rev. Lett.* **2004**, *6*, 068101.
- (6) Dąbkowska, I.; Rak, J.; Gutowski, M. *Eur. Phys. J. D* **2005**, *35*, 429–435.
- (7) Bowen, K. H., Jr., private communication.
- (8) Harańczyk, M.; Rak, J.; Gutowski, M. *J. Phys. Chem. A* **2005**, *109*, 11495–11503.
- (9) Bachorz, R. A.; Rak, J.; Gutowski, M. *Phys. Chem. Chem. Phys.* **2005**, *7*, 2116–2125.
- (10) Mazurkiewicz, K.; Bachorz, R. A.; Rak, J.; Gutowski, M. *J. Phys. Chem. B* **2006**, *110*, 24696–24707.

Thus, intramolecular proton transfer (tautomerization) may lead to the stabilization of the valence NBs anions which are not stable in their canonical forms.

Similarly, even marginal solvation, such as that originating from a single water molecule, renders the valence anions of nucleic bases adiabatically bound.¹¹ Consequently, the current view is that valence anions of isolated and canonical NBs are unbound, or at best very weakly bound, but become dominant for the solvated species.¹² Furthermore, one should bear in mind that nucleic bases in DNA interact with complementary NBs and other DNA components as well as with the cellular environment, which might further increase the stability of the initially formed anionic states.

Since the anions of nucleic bases might be the key species responsible for radiation damage of native DNA (recall that low-energy electrons are among the main products of water radiolysis¹), they have been extensively studied using both experimental^{13–17} and theoretical^{8–10,18–24} methods. Most experimental studies were devoted to pyrimidine rather than purine bases because the former are less susceptible to decomposition or isomerization in the process of transferring to the gas phase. Indeed, the only experimental result, 12 ± 5 meV, is related to the VDE of a dipole-bound anion of adenine.¹⁴ There is no experimental evidence for the occurrence of valence anions of bare adenine,¹² and only computational results are available for anionic states of isolated guanine.^{25,26} Here, it is worth noting that the electron vertical attachment energy (VAE) of adenine, measured using transmission electron spectroscopy, assumes a substantial negative value of -0.794 eV.³ The adiabatic electron affinity (AEA) for the formation of valence anions of uracil or thymine is close to zero, while their VAEs are below -0.3 eV.³ This implies that the AEA for the formation of a valence anion of adenine might be well below zero. The results of quantum chemical calculations fully account for this conclusion, as only negative values of AEA have been found, irrespective of the exchange–correlation functional and basis set used.¹²

However, interaction with solvent molecules might stabilize valence anions of adenine.^{16,17} Indeed, it was demonstrated experimentally that both water and methanol molecules stabilize the conventional anion of adenine in the gas phase.¹⁷ These

findings inspired computational studies on the anionic complexes between adenine and water or methanol.^{27,28}

An extreme consequence of strong electrostatic interactions between an anionic molecule and a ligand with proton-donating capabilities is a proton transfer from the ligand to the anionic molecule. Recently, we have described this type of process, which is induced by the attachment of an excess electron to the complex of uracil with glycine.²⁹ Here, the electron attachment leads to a barrier-free proton transfer (BFPT) from the carboxylic group of glycine to an oxygen atom of uracil, with the products being a neutral, reactive radical of hydrogenated uracil and an anion of deprotonated glycine. The BFPT process, driven by an excess electron, was confirmed in many other systems comprising a pyrimidine base and a sufficiently acidic proton donor such as an organic and inorganic acid,^{30–32} amino acid,^{33,34} and alcohol,³⁵ as well as another nucleobase.³⁶ The lack of any activation barrier to H^+ transfer indicates that this phenomenon is not kinetically controlled and thus common in anionic complexes involving a NB interacting with a proton donor. The reactive monohydroradical of a pyrimidine nucleobase, which is a typical product of the BFPT process, may trigger further chemical transformations, such as strand breaks.⁶

The stabilization of valence anions of purines in the course of intermolecular proton transfer has not been considered so far. Hence, in the present work the effect of electron attachment to the complexes of adenine (A) and 9-methyladenine (MA) with formic acid (FA) is studied. Our study is focused on valence rather than dipole-bound anions because the latter are probably irrelevant in condensed phases.¹⁸ The analysis of anionic complexes requires a basic understanding of the corresponding neutral species. Thus, our description of anions is preceded by the analysis of neutral complexes. Several possible structures of hydrogen-bonded AFA/MAFA complexes are taken into account. Next, the calculated VDE values characteristic for each anionic complex are compared to the positions of main peaks in the PES spectra. This is the way we interpret the experimental PES spectra. Finally, the possible role of purine NBs in electron-induced DNA damage is discussed.

2. Methods

2.1. Experimental Details. Negative-ion photoelectron spectroscopy (PES) is conducted by crossing a mass-selected beam of negative ions with a fixed-frequency laser beam and energy-analyzing the resultant photodetached electrons.³⁷ It is governed by the energy-conserving relationship, $h\nu = EBE + EKE$, where $h\nu$ is the photon energy, EBE

- Hendricks, J. H.; Lyapustina, S. A.; de Clercq, H. L.; Bowen, K. H. *J. Chem. Phys.* **1998**, *108*, 8–11.
- Svozil, D.; Jungwirth, P.; Havlas, Z. *Collect. Czech. Chem. Commun.* **2004**, *69*, 1395–1428.
- Hendricks, J. H.; Lyapustina, S. A.; de Clercq, H. L.; Snodgrass, J. T.; Bowen, K. H. *J. Chem. Phys.* **1996**, *104*, 7788–7791.
- Defrançois, C.; Abdoul-Carime, H.; Schermann, J. P. *J. Chem. Phys.* **1996**, *104*, 7792–7794.
- Defrançois, C.; Periquet, V.; Bouteiller, Y.; Schermann, J. P. *J. Phys. Chem. A* **1998**, *102*, 1274–1278.
- Schiedt, J.; Weinkauff, R.; Neumark, D. M.; Schlag, E. W. *Chem. Phys.* **1998**, *239*, 511–524.
- Periquet, V.; Moreau, A.; Carles, S.; Schermann, J.; Desfrancois, C. *J. Electron Spectrosc. Relat. Phenom.* **2000**, *106*, 141–151.
- Sevilla, M.; Besler, B.; Colson, A. *J. Phys. Chem.* **1995**, *99*, 1060–1063.
- Li, X.; Cai, Z.; Sevilla, M. *J. Phys. Chem. A* **2002**, *106*, 9345–9351.
- Wesolowski, S.; Leininger, M.; Pentchev, P.; Schaefer, H. *J. Am. Chem. Soc.* **2001**, *123*, 4023–4028.
- Dolgounitcheva, O.; Zakrzewski, V.; Ortiz, J. *J. Phys. Chem. A* **2001**, *105*, 8782–8786.
- Smith, D.; Jalbout, A.; Smets, J.; Adamowicz, L. *Chem. Phys.* **2000**, *260*, 45–51.
- Desfrancois, C.; Abdoul-Carime, H.; Carles, C.; Periquet, V.; Schermann, J.; Smith, D.; Adamowicz, L. *J. Chem. Phys.* **1999**, *110*, 11876–11883.
- Svozil, D.; Frigato, T.; Havlas, Z.; Jungwirth, P. *Phys. Chem. Chem. Phys.* **2005**, *7*, 840–845.
- Harańczyk, M.; Gutowski, M. *J. Am. Chem. Soc.* **2005**, *127*, 699–706.
- Harańczyk, M.; Gutowski, M. *Angew. Chem., Int. Ed.* **2005**, *44*, 6585–6587.

- Jalbout, A.; Adamowicz, L. *J. Phys. Chem. A* **2001**, *105*, 1033–1038.
- Jalbout, A.; Adamowicz, L. *J. Mol. Struct.* **2002**, *605*, 93–101.
- Gutowski, M.; Dąbkowska, I.; Rak, J.; Xu, S.; Nilles, J. M.; Radisic, D.; Bowen, K. H., Jr. *Eur. Phys. J. D* **2002**, *20*, 431–439.
- Harańczyk, M.; Bachorz, R. A.; Rak, J.; Gutowski, M.; Radisic, D.; Stokes, S. T.; Nilles, J. M.; Bowen, K. H. *J. Phys. Chem. B* **2003**, *107*, 7889–7895.
- Harańczyk, M.; Rak, J.; Gutowski, M.; Radisic, D.; Stokes, S. T.; Nilles, J. M.; Bowen, K. H. *Isr. J. Chem.* **2004**, *44*, 157–170.
- Harańczyk, M.; Dąbkowska, I.; Rak, J.; Gutowski, M.; Nilles, J. M.; Stokes, S. T.; Radisic, D.; Bowen, K. H. *J. Phys. Chem. B* **2004**, *108*, 6919–6922.
- Dąbkowska, I.; Rak, J.; Gutowski, M.; Nilles, J. M.; Radisic, D.; Bowen, K. H., Jr. *J. Chem. Phys.* **2004**, *120*, 6064–6071.
- Dąbkowska, I.; Rak, J.; Gutowski, M.; Radisic, D.; Stokes, S. T.; Nilles, J. M.; Bowen, K. H., Jr. *Phys. Chem. Chem. Phys.* **2004**, *6*, 4351–4357.
- Harańczyk, M.; Rak, J.; Gutowski, M.; Radisic, D.; Stokes, S. T.; Bowen, K. H. *J. Phys. Chem. B* **2005**, *109*, 13383–13391.
- Radisic, D.; Bowen, K. H.; Dąbkowska, I.; Storoniak, P.; Rak, J.; Gutowski, M. *J. Am. Chem. Soc.* **2005**, *127*, 6443–6450.
- Coe, J. V.; Snodgrass, J. T.; Freidhoff, C. B.; McHugh, K. M.; Bowen, K. H. *J. Chem. Phys.* **1987**, *87*, 4302–4309.

is the electron binding energy, and EKE is the electron kinetic energy. If one knows the photon energy of the experiment and one measures the electron kinetic energy spectrum, then by difference one obtains electron binding energies, which in effect are the transition energies from the anion to the various energetically accessible states of its corresponding neutral.

Our apparatus has been described elsewhere.³⁸ To prepare the species of interest, a mixture of adenine and formic acid was placed in the stagnation chamber of a nozzle source and heated to ~ 180 °C. Argon gas at a pressure of 1–2 atm was used as the expansion gas, and the nozzle diameter was 25 μm . Electrons were injected into the emerging jet expansion from a negatively biased ThO_2/Ir filament in the presence of an axial magnetic field. The resulting anions were extracted and mass-selected with a magnetic sector mass spectrometer. Electrons were then photodetached from the selected anions with ~ 100 W of circulating 2.540 eV photons and finally energy-analyzed with a hemispherical electron energy analyzer.

2.2. Computational Details. The structures of neutral complexes characterized in the current study will be labeled as A_x^yFA , where A and FA stand for adenine and formic acid, respectively, while x and y represent the adenine centers, proton acceptor (subscript), and proton donor (superscript) involved in hydrogen bonding with FA. For example, $\text{A}_{\text{N}9}^{\text{N}3}\text{FA}$ denotes a hydrogen-bonded dimer of adenine and formic acid, stabilized by two hydrogen bonds, in which the N9 atom of adenine plays the role of a proton donor while its N3 atom plays the role of a proton acceptor. The symbols of anions are preceded with an a , e.g., $a\text{A}_x^y\text{FA}$, indicating the *parent* neutral structure A_x^yFA to which the anionic structure is related. More precisely, an anionic structure $a\text{A}_x^y\text{FA}$ is determined in the course of geometry optimization initialized from the optimal geometry for the neutral structure A_x^yFA .

The stabilization energies, E_{stab} , of neutral complexes are calculated as the difference between the energy of the complex and the sum of the energies of fully optimized isolated monomers. Therefore, E_{stab} obtained in this way includes deformation energies of the monomers. The stabilization energies have been corrected for basis set superposition error (BSSE) using the counterpoise correction.^{39,40} In addition to the stabilization energies, we calculated stabilization free energies, G_{stab} . The latter result from correcting the values of E_{stab} for zero-point vibration terms, thermal contributions to energy, the pV terms, and the entropy terms. These terms were calculated in the rigid rotor–harmonic oscillator approximation for $T = 298$ K and $p = 1$ atm.

Electron vertical detachment energies—direct observables in our photoelectron spectroscopy experiments—were evaluated as the difference between the energies of the neutral and anionic complexes at the geometry of the fully relaxed anion. The difference in Gibbs free energies of the neutral complex and the anion at their corresponding fully relaxed structures is denoted EBE_G .

As our primary research method, we applied density functional theory (DFT) with Becke's three-parameter hybrid functional (B3LYP),^{41–43} In the DFT approach we employed the 6-31++G** basis set.^{44,45} Five d functions were used on heavy atoms. The usefulness of the B3LYP/6-31++G** method to describe intra- and intermolecular hydrogen bonds has been demonstrated in recent studies through comparison with the second-order Møller–Plesset (MP2) predictions.⁴⁶ The ability of the B3LYP method to predict excess electron binding energies has

recently been reviewed, and the results were found to be satisfactory for valence-type molecular anions.⁴⁷

It is known that the B3LYP method underestimates barriers for proton-transfer reactions,⁴⁸ and thus the lack of a barrier for the proton-transfer reaction may be an artifact of the B3LYP method. For this reason, we performed additional geometry optimizations using the MP2 method and the MPW1K exchange–correlation functional, which was parametrized to reproduce barrier heights for chemical reactions.⁴⁸ In the MP2 calculations we used aug-cc-pVDZ basis sets,⁴⁹ while we settled for the 6-31++G** basis set in the MPW1K approach. Finally, to strengthen our conclusion, CCSD/aug-cc-pVDZ (coupled-cluster theory with single and double excitations) calculations⁵⁰ were performed for the most stable structures of anions and neutral complexes. These single-point calculations were carried out at the optimal MP2/aug-cc-pVDZ geometries. The 1s orbitals of carbon, nitrogen, and oxygen were excluded from the MP2 and coupled-cluster treatments.

All MP2 and DFT calculations were carried out with the GAUSSIAN 03⁵¹ code on dual Intel Itanium2 nodes. The single-point CCSD calculations were performed with the Tensor Contraction Engine (TCE) of the NWChem 4.7 software package⁵² on a cluster of Intel Itanium2 nodes with the Quadrics ELAN4 interconnect. The pictures of molecules and orbitals were plotted with the Molden program.⁵³

3. Results

One can treat a photoelectron experiment for molecular complexes as a three-step process. First, the formation of neutral species of interest, in our case the A(MA)FA complexes, takes place. Then the attachment of an excess electron to the neutral species takes place. Finally, the mass-selected beam of anions is crossed with a fixed-frequency laser beam and kinetic energies of detached electrons are recorded. The properties of interest for this study, i.e., E_{stab} , AEA, and VDE, are illustrated in Figure 1. Here, formation of a neutral complex from FA and A(MA) is accompanied with an energy gain equal to E_{stab} (see Figure 1). Additional energy is then released in the process of electron attachment (AEA, see Figure 1). Finally, in a very quick process, a photon is absorbed by an anion and an excess electron is detached, which allows the vertical detachment energy to be determined (VDE, see Figure 1).

In the following, we shall discuss the results of our photoelectron experiment. Next, these data will be interpreted employing the scheme of Figure 1. First, we will report the geometric and energetic characteristics of all possible neutral complexes AFA and MAFA stabilized by two cyclic hydrogen bonds. Second, the most stable anions will be characterized, and the calculated VDE values will provide interpretation of the PES spectra.

3.1. PES Spectra of Anionic Complexes of Adenine and 9-Methyladenine with Formic Acid. Photoelectron spectra depicted in Figure 2 indicate that the AFA and MAFA complexes form stable anions. Isolated adenine does not support bound valence anions in the gas phase.¹² So far, only the

- (38) Coe, J. V.; Snodgrass, J. T.; Freidhoff, C. B.; McHugh, K. M.; Bowen, K. H. *J. Chem. Phys.* **1986**, *84*, 618–625.
 (39) Boys, S. F.; Bernardi, F. *Mol. Phys.* **1970**, *19*, 553–566.
 (40) Gutowski, M.; Chalasinski, G. *J. Chem. Phys.* **1993**, *98*, 5540–5554.
 (41) Becke, A. D. *Phys. Rev. A* **1988**, *38*, 3098–3100.
 (42) Becke, A. D. *J. Chem. Phys.* **1993**, *98*, 5648–5652.
 (43) Lee, C.; Yang, W.; Paar, R. G. *Phys. Rev. B* **1988**, *37*, 785–789.
 (44) Ditchfield, R.; Hehre, W. J.; Pople, J. A. *J. Chem. Phys.* **1971**, *54*, 724–728.
 (45) Hehre, W. J.; Ditchfield, R.; Pople, J. A. *J. Chem. Phys.* **1972**, *56*, 2257–2261.
 (46) van Mourik, T.; Price, S. L.; Clary, D. C. *J. Phys. Chem. A* **1999**, *103*, 1611–1618.

- (47) Rienstra-Kiracofe, J. C.; Tschumper, G. S.; Schaefer, H. F., III, *Chem. Rev.* **2002**, *102*, 231–282.
 (48) Lynch, B. J.; Fast, P. L.; Harris, M.; Truhlar, D. G. *J. Phys. Chem. A* **2000**, *104*, 4811–4815.
 (49) Kendall, R. A.; Dunning, T. H., Jr.; Harrison, R. J. *J. Chem. Phys.* **1992**, *96*, 7696–7709.
 (50) Taylor, P. R. In *Lecture Notes in Quantum Chemistry II*; Roos, B. O., Ed.; Springer-Verlag: Berlin, 1994.
 (51) Frisch, M. J.; et al. *Gaussian 03*, Revision C.02; Gaussian, Inc.: Pittsburgh PA, 1998.
 (52) Aprà, E.; et al. *NWChem, A Computational Chemistry Package for Parallel Computers*, Version 4.7; PNNL: Richland, WA, 2004.
 (53) Schaftenaar, G.; Noordik, J. H. *J. Comput.-Aided Mol. Design* **2000**, *14*, 123–134.

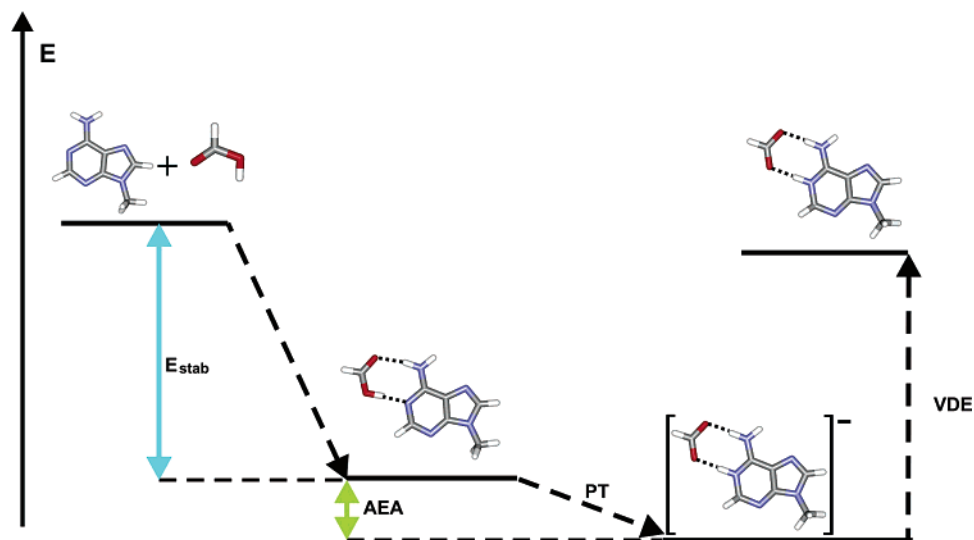


Figure 1. Illustration of E_{stab} , AEA, and VDE.

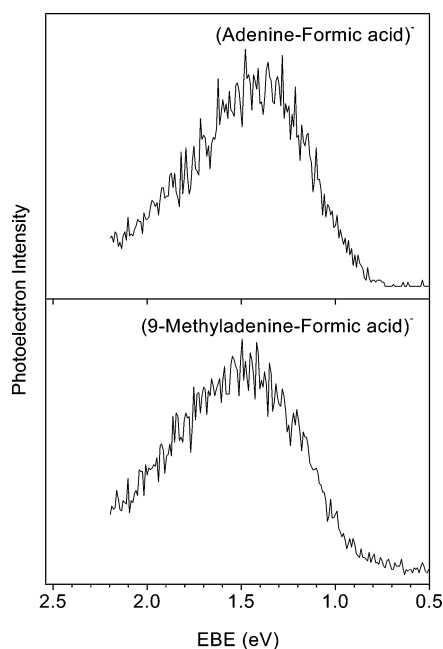


Figure 2. Photoelectron spectrum of adenine–formic acid (upper graph) and 9-methyladenine–formic acid anions (lower graph) measured with 2.54 eV electrons.

existence of the dipole-bound anions¹⁴ and metastable shape resonances³ of adenine has been reported. The dipole moment of adenine calculated at the MP2/aug-cc-pVDZ level amounts to 2.56 D,⁵⁴ and that of FA, obtained at the B3LYP/TZVP+ level, equals 1.74 D.⁵⁵ Even if one assumed an ideal alignment of the dipole moments of FA and A (which is electrostatically highly improbable), the total dipole moment of 4.3 D would provide the binding energy of the resulting dipole-bound state on the order of 50–90 meV (recall that the MP2/aug-cc-pVDZ dipole moment of uracil amounts to 4.38 D and the calculated VDE is 73 meV⁹). Therefore, the maxima in the PES spectra displayed in Figure 2 are at much too large electron binding energies to be ascribed to dipole-bound states. Moreover, the

PES spectra of dipole-bound anions of NBs are dominated by narrow and sharp peaks and low electron binding energies. On the other hand, the PES spectra of anionic complexes, in which a NB interacts with a proton donor molecule and an excess electron is localized on a π^* orbital, typically spread over a range of 1 eV, with the maximum intensity between 1 and 2 eV. Indeed, the spectra displayed in Figure 2 cover broad ranges of binding energies, 1.0–2.0 eV, with a maximum at 1.45 and 1.50 eV for the AFA[−] and MAFA[−] complexes, respectively. Hence, they correspond to stable valence anions rather than to dipole-bound states.

In these valence anions, an excess electron might be localized on the A(MA) or FA molecule. In the former case, the system would represent a valence anion, A[−](MA[−]), solvated by FA, while in the latter case the situation would be reversed—a molecule of adenine would solvate FA[−]. Recently, we have demonstrated that formic acid forms vertically stable valence anions when solvated by another molecule of FA.⁵⁵ The resulting (FA)₂[−] complex undergoes BFPT; i.e., a proton is transferred to the unit where the unpaired electron is localized, and the calculated VDE is 2.5 eV. On the other hand, the VDE would be only 1 eV if the intermolecular proton transfer did not occur. This information and the measured VDEs of 1.50 and 1.45 eV for AFA[−] and MAFA[−], respectively, will help us to resolve whether the excess electron is localized on A(MA) or on FA.

Let us assume that the excess electron is localized on FA. If there was no proton transfer from A(MA) to FA[−], the resulting VDE would probably be smaller than 1.0 eV, because adenine is a weaker acid than FA. The measured VDE values of 1.50 and 1.45 eV are inconsistent with this scenario. On the other hand, if there was a proton transfer from A(MA) to FA[−], then the resulting VDE would probably be larger than 2 eV, which is again inconsistent with the measured VDE values. Thus, the PES spectra displayed in Figure 2 must originate from valence anions in which an excess electron is localized on adenine. Moreover, the measured values of VDE for AFA and MAFA are comparable to those measured for complexes of pyrimidine bases with proton donors, in which intermolecular proton transfer induced by electron attachment occurs. Indeed, the following computational results suggest that BFPT takes place in the AFA[−] and MAFA[−] systems.

(54) Sponer, J.; Leszczynski, J.; Hobza, P. *Biopolymers* **2001**, *61*, 3–31.

(55) Bachorz, R. A.; Harańczyk, M.; Dąbkowska, I.; Rak, J.; Gutowski, M. *J. Chem. Phys.* **2005**, *122*, 204304.

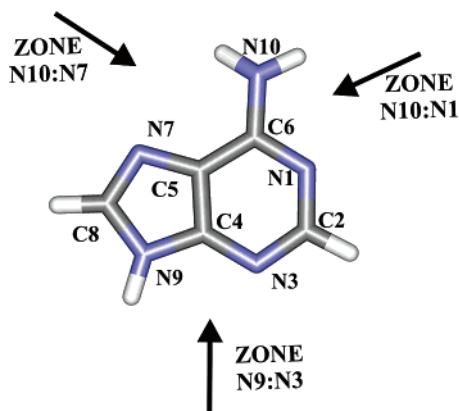


Figure 3. Regions of adenine capable of forming two hydrogen bonds with a molecule of formic acid.

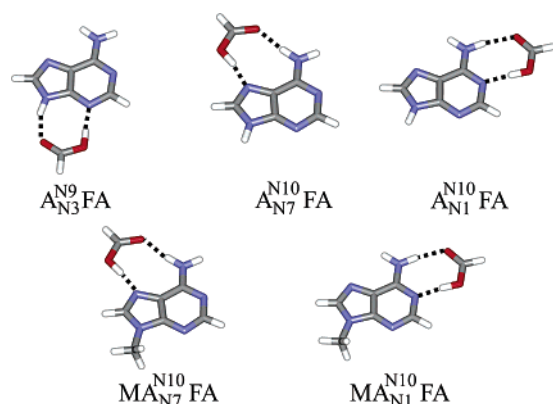


Figure 4. Neutral AFA and MAFA complexes.

3.2. Computational Results. 3.2.1. Neutral Complexes. The equilibrium geometries of various complexes between adenine and formic acid are governed by hydrogen bonding. The conformational space for the species interacting via a single hydrogen bond is complex, but these structures are disfavored compared to cyclic geometries where two hydrogen bonds are operative. Therefore, we will limit our further discussion to the more stable cyclic dimers.

Adenine has three regions capable of forming two hydrogen bonds with FA (see Figure 3). The complexes in which the N10: N1 and N10:N7 atoms are involved in hydrogen bonds will be dubbed Watson–Crick and Hoogsteen, respectively, since these patterns of hydrogen bonding are characteristic for the Watson–Crick and Hoogsteen complexes between complementary nucleobases, respectively. The third complex, where FA interacts with the N9 and N3 atoms of adenine, does not have an equivalent within the naturally occurring pairs of NBs because the N9 site is engaged in a chemical bond with a sugar unit.

The strength of a hydrogen bond is determined by (i) the charge distribution in the proton donor (YH) and acceptor (X) fragments, (ii) the distance between H and X, and (iii) the $X\cdots HY$ angle. A preference for nearly linear hydrogen bonds is well established, as was demonstrated for a variety of systems. The cyclic structures of neutral complexes between A and FA are displayed in the upper part of Figure 4. All complexes are stabilized by two strong hydrogen bonds, as indicated by the H-bonds characteristics gathered in Table S1 (Supporting Information). Indeed, the hydrogen bond lengths span a range of 1.66–1.90 Å and the $X\cdots HY$ angles span a range of 155–

Table 1. Values of Stabilization Energy (E_{stab}) and Stabilization Free Energy (G_{stab}) as Well as Their Relative Values (ΔE and ΔG) for the Neutral Adenine–Formic Acid and 9-Methyladenine–Formic Acid Complexes, Calculated at the B3LYP/6-31++G** Level (All Values in kcal/mol)

complex	E_{stab}^a	ΔE	G_{stab}	ΔG
Adenine–Formic Acid				
$A_{N_{10}}^{N_{10}}$ FA	−15.84 (−15.13)	1.83	−2.01	2.11
$A_{N_{10}}^{N_{10}}$ FA	−15.28 (−14.45)	2.40	−1.35	2.77
$A_{N_9}^{N_9}$ FA	−17.67 (−16.83)	0	−4.11	0
9-Methyladenine–Formic Acid				
$MA_{N_{10}}^{N_{10}}$ FA	−15.66 (−14.82)	0.30	−2.09	0.59
$MA_{N_1}^{N_{10}}$ FA	−15.96 (−15.26)	0	−2.68	0

^a Values corrected for BSSE are given in parentheses.

178° (see Table S1). The hydrogen bonds show a substantial asymmetry; the hydrogen bond which involves a proton donor center of adenine is shorter by 0.15–0.25 Å compared with the second hydrogen bond. Analyzing the geometrical data displayed in Table S1, one can conclude that the Hoogsteen dimer is probably the least stable structure, whereas $A_{N_{10}}^{N_{10}}$ FA and $A_{N_9}^{N_9}$ FA are probably of similar stability. Table 1 summarizes energetic characteristics of the adenine–formic acid complexes. The B3LYP stabilizations energies span a range of −15.1 to −16.8 kcal/mol, indicating strong interactions between the monomers. The outcome of the qualitative analysis regarding the geometry of hydrogen bonds is reflected in the energetic order of complexes under consideration. Indeed, the Hoogsteen complex $A_{N_7}^{N_{10}}$ FA is the least stable and the Watson–Crick complex is less stable than $A_{N_3}^{N_9}$ FA by less than 2 kcal/mol (see Table 1). The strength of hydrogen bonds typically correlates with the proton affinity (PA) of the proton acceptor and the deprotonation enthalpy (DPE) of the proton donor.⁵⁶ This also holds for the complexes studied in the current work. Namely, an exceptionally low DPE of N9–H (see Table S2, Supporting Information) accounts for the highest stability of the $A_{N_3}^{N_9}$ FA dimer (see Table 1). Furthermore, a low PA of N7 (see Table S2) explains the lower stability of the Hoogsteen complex with respect to the Watson–Crick complex (see Table 1).

The free energies of stabilization are negative for all studied complexes; thus, their formation should be spontaneous. Using the relative values of ΔG (see Table 1), one can calculate (for details, see ref 34) that, in the gaseous mixture of adenine and formic acid at 298 K, the molar ratio $A_{N_3}^{N_9}$ FA: $A_{N_{10}}^{N_{10}}$ FA: $A_{N_7}^{N_{10}}$ FA equals 0.964:0.027:0.009. Consequently, the mixture is dominated by the $A_{N_3}^{N_9}$ FA complexes in the gas phase.

Only Watson–Crick- and Hoogsteen-type cyclic complexes can be formed between 9-methyladenine and FA (see the bottom part of Figure 4). The N1:N9 region (see Figure 1) of MA cannot be involved in hydrogen bonding because the N9 site is methylated. The geometric characteristics of hydrogen bonds in the MAFA complexes are very similar to those found in the AFA structures (cf. Table S1). A substantial asymmetry between the two hydrogen bonds also is observed. Thus, the presence of a methyl group at N9 exerts only minor effects on the adenine's propensity to form hydrogen-bonded structures. Taking into account the data gathered in Table S1, one can predict that $MA_{N_{10}}^{N_{10}}$ FA should be the most stable structure (notice a shorter N1 \cdots HO bond in $MA_{N_{10}}^{N_{10}}$ FA compared with

(56) Dąbkowska, I.; Rak, J.; Gutowski, M. *J. Phys. Chem. A* **2002**, *106*, 7423–7433.

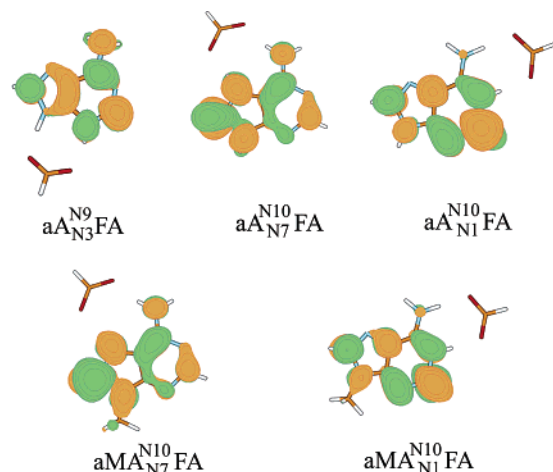


Figure 5. Anionic AFA and MAFA complexes and their singly occupied molecular orbital plotted with a spacing 0.03 bohr^{-3/2}.

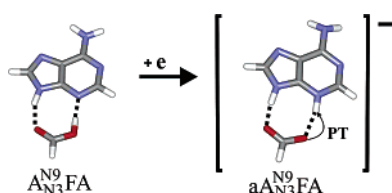


Figure 6. Example of barrier-free proton-transfer reaction induced by excess electron attachment.

N7···OH in MA_{N₇}^{N₁₀}FA and almost identical parameters for the second hydrogen bond; see Table S1). Indeed, MA_{N₁}^{N₁₀}FA is more stable than MA_{N₇}^{N₁₀}FA (see Table 1). However, despite the significant difference in the PA characteristics for the proton-acceptor centers, and hence in the strength of the hydrogen bonds, the stabilization energies, and in consequence the relative stabilities, differ only marginally. Clearly, the strength of hydrogen bonds alone does not account for the energetics of the structures discussed.

The free energies of stabilization for MA_{N₁}^{N₁₀}FA and MA_{N₇}^{N₁₀}FA are negative (see Table 1), and consequently the dimerization should take place spontaneously at 298 K. In contrast to the AFA dimers, where A_{N₃}^{N₉}FA dominates in the gas phase, the MA_{N₁}^{N₁₀}FA and MA_{N₇}^{N₁₀}FA complexes should coexist, as indicated by the molar ratio 0.563:0.437 calculated on the basis of the respective free energies.

3.2.2. Anionic Complexes. Attachment of an electron to the AFA and MAFA complexes leads to the formation of stable valence anions (see Figure 1). A common feature of the anionic wave function identified by us is that the excess electron is localized on a π^* orbital of adenine (see Figure 5), which is consistent with the conclusion drawn on the basis of the experimental PES spectra. Moreover, attachment of an excess electron leads to spontaneous proton transfer from the OH group of FA to a proton-acceptor site of A(MA). For clarity, an example of such a reaction is depicted in Figure 6. Since the B3LYP method predicts too low kinetic barriers, we checked the occurrence of proton transfer using more reliable computational models. It turned out that the PT reaction is predicted to be barrier-free also at the MPW1K and MP2 levels, which strengthens our conclusion.

A driving force for the BFPT process is stabilization of the excess electron on a π^* orbital of the anionic adenine. Contrary

Table 2. Values of Relative Electronic Energy and Free Energy (ΔE and ΔG) with Respect to the Most Stable Anion, Adiabatic Electron Affinity (AEA_G), and Electron Vertical Detachment Energy (VDE) for the Anionic Adenine–Formic Acid and 9-Methyladenine–Formic Acid Complexes Calculated at the B3LYP/6-31++G** Level (ΔE and ΔG in kcal/mol; AEA_G and VDE in eV)

anion	ΔE	ΔG	AEA _G	VDE
Adenine–Formic Acid				
aA _{N₁} ^{N₁₀} FA	9.61	9.41	0.36	1.09
aA _{N₇} ^{N₁₀} FA	3.63	4.62	0.59	1.84
aA _{N₃} ^{N₉} FA	0	0	0.67	1.21
9-Methyladenine–Formic Acid				
aMA _{N₁} ^{N₁₀} FA	5.95	4.15	0.34	0.96
aMA _{N₇} ^{N₁₀} FA	0	0	0.54	1.67

to the anionic complexes of pyrimidine bases with FA,³² all anionic AFA and MAFA complexes identified in the current work undergo BFPT. The excess electron is distributed evenly over the proton-acceptor centers in adenine. In pyrimidines, on the other hand, the excess electron distribution is highly asymmetric, which explains why only certain complexes of pyrimidines are susceptible to BFPT.

In Table S3 (Supporting Information), the geometric characteristics of hydrogen bonds that stabilize the anionic structures are summarized. The hydrogen bond lengths span a range of 1.67–1.81 Å, and the X···HY angles span a range of 164–178° (see Table S3). On average, the hydrogen bonds for anions are shorter and more linear than those identified in the neutral complexes (cf. Tables S1 and S3). The shortest H···X distances, 1.674 and 1.695 Å, occur in the aA_{N₃}^{N₉}FA and aMA_{N₇}^{N₁₀}FA dimers, respectively, which implies that these two systems might be the most stable. This conclusion is indeed confirmed by the values of relative electronic energies as well as free energies displayed in Table 2.

All anions identified by us are adiabatically stable by 0.3–0.7 eV with respect to the neutral complexes (see the AEA_G values in Table 2). Besides the experimental work of Desfrancois et al.,¹⁷ who reported that two molecules of water and three molecules of methanol are sufficient to stabilize the valence anion of adenine, all earlier reports indicated a significant instability of gas-phase valence anions of adenine. Only dipole-bound anions were characterized in an earlier computational study by Jalbout and Adamowicz on [A···(H₂O)_n]⁻.²⁷ The results reported by the same authors on valence anions of [A···(CH₃OH)_n]⁻ ($n \leq 3$) were inconclusive.²⁸ Thus, the results presented in the current study can be considered as the first theoretical–experimental confirmation of the existence of stable valence anionic complexes of adenine with a proton-donating moiety, in which the unpaired electron is localized on adenine. The stability of the A(MA)FA⁻ complexes is enhanced by the intermolecular proton transfer.

In complexes of pyrimidine bases with proton-donating moieties, the relative stabilities of neutral and anionic isomers were frequently very different.²⁹ In other words, the most stable anionic complexes do not originate from the most stable neutral complexes. Here, the most stable anion, aA_{N₃}^{N₉}FA, is related to the most stable neutral complex (see Tables 1 and 2). However, this observation does not hold for the MAFA complexes, where the most stable anion, aMA_{N₇}^{N₁₀}FA, corresponds to the least stable neutral (cf. Tables 1 and 2). Attachment of an electron increases the relative stability of the A_{N₃}^{N₉}FA and MA_{N₇}^{N₁₀}FA

Table 3. VDE for Anionic Complexes Calculated with Various Theoretical Models (All Values in eV)

anion	model ^a			C(inc)
	A	B	C	
Adenine–Formic Acid				
$aA_{N_{10}}^{N_{10}}FA$	1.09	1.01	1.38	1.18
$aA_{N_{10}}^{N_{7}}FA$	1.84	1.53	1.91	1.71
$aA_{N_{3}}^{N_{9}}FA$	1.21	1.38	1.70	1.50
9-Methyladenine–Formic Acid				
$aMA_{N_{10}}^{N_{10}}FA$	0.96	0.94	1.38	1.18
$aMA_{N_{7}}^{N_{10}}FA$	1.67	1.36	1.75	1.55

^a A, B, and C stand for B3LYP/6-31++G**, MP2/aug-cc-pVDZ, and B3LYP/6-31++G**//MP2/aug-cc-pVDZ, respectively. C(inc) stands for C incremented with -0.2 eV.

structures with respect to the remaining structures. As a result, a gaseous sample of anionic species is expected to be dominated by the lowest energy isomers. The relative free energies (see Table 2) lead to molar ratios of 9.996×10^{-1} : 4.089×10^{-4} : 1.260×10^{-7} and 9.991×10^{-1} : 9.040×10^{-4} for $[aA_{N_{3}}^{N_{9}}FA]:[aA_{N_{7}}^{N_{10}}FA]:[aA_{N_{10}}^{N_{10}}FA]$ and $[aMA_{N_{7}}^{N_{10}}FA]:[aMA_{N_{10}}^{N_{10}}FA]$, respectively.

Next we compare the calculated vertical detachment energies with the experimental findings. The VDEs estimated using four computational models (B3LYP, MP2, B3LYP//MP2, and B3LYP//MP2 incremented with -0.2 eV) are contrasted in Table 3. In the past, we found that the VDE values calculated using the B3LYP methods is typically overestimated by ca. 0.2 eV for valence anions of heteroaromatic species.²⁹ The same shift by -0.2 eV works pretty well also for the MAFA anions studied in this work. The B3LYP values of VDE estimated for $aMA_{N_{10}}^{N_{10}}FA$ and $aMA_{N_{7}}^{N_{10}}FA$ are equal to 0.96 and 1.67 eV, respectively (see Table 3). Applying an increment of -0.2 eV, one obtains 0.76 and 1.47 eV, respectively. As was shown above, a gaseous sample of MAFA⁻ contains exclusively the $aMA_{N_{7}}^{N_{10}}FA$ species. Thus, one can predict that the maximum of the PES spectrum for the anions of MAFA should appear at ca. 1.5 eV, which, indeed, falls in the region displayed in Figure 2.

The situation is different for the anionic AFA complexes. The B3LYP VDEs were calculated to be 1.09, 1.84, and 1.21 eV for $aA_{N_{10}}^{N_{10}}FA$, $aA_{N_{7}}^{N_{10}}FA$, and $aA_{N_{3}}^{N_{9}}FA$, respectively, and the corresponding VDEs incremented by -0.2 eV would be 0.89, 1.64, and 1.01 eV. The maximum of the dominant PES feature is at 1.45 eV (see Figure 2). Thus, none of the calculated values is consistent with the measured spectrum. Although the MP2 VDE value for $aA_{N_{7}}^{N_{10}}FA$ is close to the experimental value (see Table 3), one should remember that this species is not represented in the gas phase. On the other hand, the MP2 VDE value for the most stable anion, $aA_{N_{3}}^{N_{9}}FA$, amounts to 1.38 eV, which is consistent with our previous finding that the MP2 values are typically underestimated.³⁵ The inconclusive B3LYP results prompted us to carry out additional calculations of VDE at the CCSD/aug-cc-pVDZ level using anionic geometries optimized at the MP2/aug-cc-pVDZ level. These computationally very demanding results were obtained only for the most stable isomers of AFA⁻ and MAFA⁻. The resulting CCSD values of VDE are 1.56 and 1.59 eV for $aA_{N_{3}}^{N_{9}}FA$ and $aMA_{N_{7}}^{N_{10}}FA$, respectively. These values match the positions of the PES peaks in Figure 2 better than the results obtained at the

B3LYP or MP2 levels, although they seem to be somewhat overestimated.

A close inspection of anionic geometries determined at the B3LYP and MP2 levels reveals particularly significant differences for $aA_{N_{3}}^{N_{9}}FA$. Namely, the ring of adenine is much more buckled at the MP2 than at the B3LYP level (see Table S4, Supporting Information). This effect is probably related to an artificial delocalization of the electronic charge predicted by the DFT methods.⁵⁷ In line with this finding, we recalculated all VDEs at the B3LYP level using the optimal anionic MP2 geometries (see Table 3, model C). Next, the VDE values obtained using model C were incremented by -0.2 eV, and the results are reported in the last column of Table 3. The VDE for the most stable anion, $aA_{N_{3}}^{N_{9}}FA$, amounts to 1.50 eV and differs by only $+0.05$ eV from the observed value and by -0.06 eV from the CCSD/aug-cc-pVDZ value. Similarly, the analogous estimate of VDE for $aMA_{N_{7}}^{N_{10}}FA$ is only 0.05 eV above the experimental value. It is also worth noting that the experimental difference between the VDEs for $aA_{N_{3}}^{N_{9}}FA$ and $aMA_{N_{7}}^{N_{10}}FA$ (0.05 eV) is well reproduced within this model. Thus, the problem of calculating reliable VDEs for the AFA⁻ complexes has been traced back to the deficiency of the B3LYP method to predict correct geometries for valence anions.

This finding prompted us to build a statistical model which could correct the deficiency of the B3LYP method and render reliable estimates of VDE. In order to make this model general, we used most of the experimental and theoretical data published so far for the BFPT systems (see Table S4). The proposed correlation equation for VDE depends on two parameters only: the B3LYP value of VDE and the difference in nonplanarity (ΔNP) of a nucleobase predicted at the B3LYP and MP2 levels. For each complex, we determined the nonplanarity of a nucleobase on the basis of the geometry of its conjugated ring only. The NP is given by the sum of distances between heavy atoms in the ring and a plane determined by the same set of heavy atoms. The plane is determined in the standard least-squares procedure. In this way we ended up with the following equation:

$$VDE = a(\Delta NP)^2 + VDE(B3LYP) + b \quad (1)$$

where a and b are correlation coefficients. In this model, an increase in the VDE value in comparison with the B3LYP result depends in a harmonic fashion on ΔNP . From the data displayed in Table S4, the values of a and b and the square of the regression coefficient were found to be 31.92 ± 4.45 , -0.107 ± 0.017 , and 0.960, respectively. A reasonable quality of the fit demonstrates the predictive power of eq 1, showing simultaneously that the overestimation of planarity explains the deficiency of the B3LYP model. It is worth noticing that the b parameter amounts to -0.11 eV, which is close to the increment of -0.2 eV used in the BFPT studies carried out so far. Since the model uses only B3LYP and MP2 data, it is much cheaper than the relatively accurate CCSD approach. Thus, the general recipe enabling a reliable estimation of VDE for this type of anions can be realized within a four-step procedure: (i) identification of the lowest energy anionic structure using an inexpensive B3LYP/6-31++G** model, (ii) re-optimization of this structure employing the MP2/aug-cc-pVDZ method, (iii)

(57) Bally, T.; Sastry, G. N. *J. Phys. Chem. A* **1997**, *101*, 7923–7925.

calculation of the difference in planarity between the B3LYP and MP2 structures, and finally (iv) the prediction of VDE using eq 1. An alternative approach would be to shift the MP2 values of VDE for anionic complexes using information about the CCSD(T) and MP2 values of VDE obtained for isolated NBs.

4. Discussion

The current study demonstrates unequivocally that adenine and 9-methyladenine are capable of forming stable valence anions in complexes with sufficiently strong proton donors. The adiabatic electron affinities of the AFA and MAFA complexes span a range of 0.36–0.67 eV. We identified barrier-free intermolecular proton transfer in these anionic complexes, which enhances their stability. Indeed, the AEA of nucleotides of thymine and cytosine, which are believed to have larger affinity toward electron binding than adenine, were calculated to be only 0.56 and 0.44 eV at the B3LYP/DZP++ level for the 3'-monophosphates of thymine and cytosine, respectively.⁵⁸

The products of the intermolecular proton-transfer reactions studied in the present work are the neutral radical AH[•]/MAH[•] and the deprotonated formic acid. If formed in DNA, the former species might react with an adjacent deoxyribose molecule, triggering strand breaks.⁶ However, so far, only pyrimidine bases were considered to be directly involved in the DNA damage induced by low-energy electrons.⁵⁹ The assumption was based on an electron affinity sequence assumed for isolated NBs: T ≈ C > A > G.⁶⁰ This sequence suggests that thymine and cytosine molecules should be primary targets for the formation of nucleic base anions in DNA. One should, however, realize that in contrast to pyrimidine bases, purine molecules possess proton-donor and -acceptor centers that are not involved, or are only partially involved, in the Watson–Crick pairing scheme and may therefore form additional hydrogen bonds. Indeed, this type of interaction is responsible for the formation of the so-called DNA triplexes (here, an additional pyrimidine strand is attached to a purine strand in the regular DNA duplex), e.g., through the Hoogsteen pairing scheme.⁶¹ The intermolecular interactions that develop through the above-mentioned proton-donor and -acceptor centers of purines may contribute to the stability of valence anions and alter the ordering of electron affinities observed in isolated nucleic bases.

The interaction between anionic purines and amino acids or amino acid side chains (e.g., via the Hoogsteen scheme) might counterbalance the larger AEAs of isolated pyrimidines. If so, then both types of NBs could play a significant role in DNA damage induced by low-energy electrons. Here, it should be borne in mind that, in the cellular environment, DNA interacts with many types of proteins, like replication and repair enzymes and histones. We inspected interactions published in an amino acid–nucleotide database (AANT) containing crystallographic structures for 1213 protein–nucleic acids complexes⁶² and found that the purine–amino acid side chain contacts account for the majority of the interactions. Namely, out of 3066 contacts

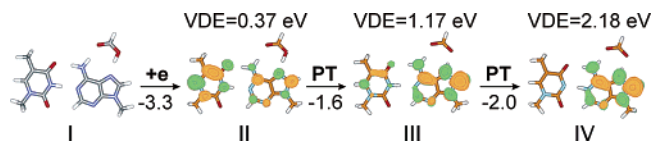


Figure 7. Electron binding to the Watson–Crick MAMT base pair solvated by formic acid at the Hoogsteen site (I). As a consequence of intermolecular proton transfers, the radicals MAH[•] (III) and MAH₂^{•+} (IV) are formed, and the unpaired electron becomes localized on 9-methyladenine. Both the initial electron attachment and the following two intermolecular proton transfers are thermodynamically favorable, and the accompanying changes in B3LYP electronic energies are given below the arrows in kilocalories per mole.

between nucleobases and amino acid side chains, 43.7% and 21.4% involve guanine and adenine, respectively. As demonstrated in the current work, the presence of formic acid renders the valence anion of adenine and 9-methyladenine exceptionally stable. In the cellular environment, adenine may interact, for example, with the side chain of arginine, which at physiological pH is protonated. Indeed, analysis of the AANT database indicates that the Hoogsteen-type interactions between adenine and charged arginine account for the majority of adenine–amino acid side chain contacts. Attachment of an electron to adenine (as well as to guanine) complexed with charged arginine might induce BFPT (similar to the BFPT predicted in the anions of AFA and MAFA), and the reactive neutral AH[•] radical might initiate a sequence of processes leading to a single strand break.

We have recently initiated a systematic computational and experimental study of the anionic 9-methyladenine–1-methylthymine–formic acid trimer, MAMTFA[−], with the main purpose being to understand how the presence of FA affects the binding of the excess electron by the MAMT pair. Here we report our computational B3LYP/6-31+G** results for one specific hydrogen-bonded system, in which the Watson–Crick MAMT pair forms a cyclic hydrogen-bonded structure with FA through the Hoogsteen sites of MA, i.e., N7 and N10H (see Figure 7). Attachment of an excess electron to this trimer leads to an anionic structure with an unpaired electron localized primarily on thymine and characterized by a VDE of 0.37 eV. This localization of the unpaired electron is consistent with the sequence of electron affinities of isolated NBs: T > A.⁶⁰ The anionic structure is, however, only a local minimum on the potential energy surface of the anionic trimer. The values of proton affinities and deprotonation enthalpies for the relevant sites of neutral adenine and thymine suggest that intermolecular proton transfer from thymine to adenine is feasible (see Table 3 and ref 36). Indeed, two consecutive intermolecular proton transfers are thermodynamically favorable and lead to (1) an intermediate anionic trimer built of MAH[•], deprotonated FA, and MT, and (2) the global minimum structure built of MAH₂^{•+}, deprotonated FA, and deprotonated MT. As a consequence of two intermolecular proton transfers, the excess electron is localized exclusively on adenine, and the VDE is as large as 2.21 eV. Thus, our computational result suggests that, if adenine in DNA interacts with an amino acid of a sufficiently high acidity, then an intermolecular proton transfer might occur and the unpaired electron becomes localized on adenine. A complete report from the MAMTFA[−] study will be presented elsewhere.

Computational studies on strand breaks in DNA induced by low-energy electrons have so far been focused on DNA fragments with pyrimidines.^{6,59} We suggest that further under-

(58) Gu, J.; Wang, J.; Leszczynski, J. *J. Am. Chem. Soc.* **2006**, *128*, 9322–9323.

(59) Barrios, R.; Skurski, P.; Simons, J. *J. Phys. Chem. B* **2002**, *106*, 7991–7994.

(60) Seidel, C. A. M.; Schulz, A.; Sauer, M. H. M. *J. Phys. Chem.* **1996**, *100*, 5541–5553.

(61) Kawai, K.; Saito, L. *Tetrahedron Lett.* **1998**, *39*, 5221–5224.

(62) Hoffman, M. M.; Kharpov, M. A.; Cox, J. C.; Yao, J.; Tong, J.; Ellington, A. D. *Nucleic Acids Res.* **2004**, *32*, D174–D181.

standing of DNA damage might require experimental and computational studies of DNA fragments in which purines are engaged in hydrogen bonding with proton-donating molecules through these sites that are not involved in the Watson–Crick pairing scheme.

5. Summary

The photoelectron spectra of complexes between adenine/9-methyladenine and formic acid display a broad feature characteristic for the valence-bound anions. The maxima of experimental bands measured at 1.45 and 1.50 eV for AFA and MAFA, respectively, are well reproduced by the VDEs calculated for the most stable anionic structures, $aA_{N_3}^{N_9}FA$ and $aM_{N_7}^{N_{10}}FA$.

The neutral complexes are stabilized by two strong hydrogen bonds, and the stabilization energies span a range of -15.7 to -17.7 kcal/mol. The energetic ordering of the neutral complexes usually correlates with the PA and DPE of these adenine sites that are involved in hydrogen bonds with formic acid. The relative free energies allowed the molar ratios for particular complexes to be calculated at 298 K. The gaseous mixtures of AFA is dominated by the isomer $A_{N_3}^{N_9}FA$, whereas both $M_{N_7}^{N_{10}}FA$ and $MA_{N_7}^{N_{10}}FA$ appear in comparable amounts for MAFA.

All valence anions characterized for cyclic hydrogen-bonded complexes proved to be adiabatically bound. The excess electron localizes on a π^* orbital of adenine or 9-methyladenine. Additionally, the process of electron attachment induces barrier-free proton transfer between the OH group of FA and a proton-acceptor site of adenine (9-methyladenine). The BFPT provides an additional stabilization, which explains the unexpectedly high adiabatic stability of the valence anions of AFA and MAFA. The relative free energies of stabilization indicate that only the most stable anions, i.e., $aA_{N_3}^{N_9}FA$ and $aMA_{N_7}^{N_{10}}FA$, occur in the gas phase at 298 K.

The problem of calculating reliable VDEs for the AFA complexes at the B3LYP level of theory has been traced back to the deficiency of the method to predict reliable geometries for certain anionic configurations. We proposed a statistical model which corrects the B3LYP deficiency and renders more accurate values of the VDE than the B3LYP method. The correlation equation uses the VDE calculated at the B3LYP level and the difference in nonplanarities of the NB predicted at the B3LYP and MP2 levels. The usefulness of this model was

demonstrated for a set of data published for the valence anions of pyrimidine-based complexes.

Last, we demonstrated that the radicals MAH^\bullet and $MAH_2^{+\bullet}$ might be formed upon attachment of an excess electron to MA involved in the Watson–Crick interaction with MT and solvated by FA at the Hoogsteen sites. The radicals of hydrogenated purine bases may be relevant to the DNA damage by low-energy electrons. Thus, important issues for future studies are to (i) characterize the propensity of guanine to BFPT in anionic complexes with species that mimic interactions present in DNA–protein complexes and (ii) explore whether radicals of hydrogenated purines may react with an adjacent deoxyribose molecule, triggering strand breaks in DNA.

Acknowledgment. The authors thank Dr. Piotr Storonik for valuable technical assistance. This work was supported by (i) the Polish State Committee for Scientific Research (KBN) grants BW/8000-5-0305-6 (J.R.) and KBN/1T09A04930 (K.M.), (ii) European Social Funds (EFS) ZPORR/2.22/II/2.6/ARP/U/2/05 (M.H.), (iii) the U.S. DOE Office of Biological and Environmental Research, Low Dose Radiation Research Program (M.G.), and (iv) the National Science Foundation under grant no. CHE-0517337 (K.B.). M.H. holds the Foundation for Polish Science (FNP) award for young scientists. The calculations were performed at the Academic Computer Center in Gdańsk (TASK) and at the Molecular Science Computing Facility (MSCF) in the William R. Wiley Environmental Molecular Sciences Laboratory, a national scientific user facility sponsored by the U.S. Department of Energy's Office of Biological and Environmental Research and located at the Pacific Northwest National Laboratory, which is operated by Battelle for the U.S. Department of Energy. The MSCF resources were available through a Computational Grand Challenge Application grant.

Supporting Information Available: Selected geometrical characteristics of hydrogen bonds in the neutral and anionic complexes of adenine and 9-methyladenine with formic acid; proton affinities of the N atoms and deprotonation energies of the NH bonds for selected sites of adenine; differences in nonplanarities of nucleobases rings calculated at the B3LYP and MP2 levels together with the values of measured and calculated (B3LYP) VDEs for selected BFPT systems; complete refs 51 and 52. This material is available free of charge via the Internet at <http://pubs.acs.org>.

JA066229H